Implementation of the refined Deutsch-Jozsa algorithm on a three-bit NMR quantum computer

Jaehyun Kim, Jae-Seung Lee, and Soonchil Lee
Department of Physics, Korea Advanced Institute of Science and Technology, Taejon, 305-701, Korea

Chaejoon Cheong
Magnetic Resonance Team, Korea Basic Science Institute, Taejon, 305-333, Korea
(Received 14 January 2000; published 19 July 2000)

We implemented the refined Deutsch-Jozsa algorithm on a three-bit nuclear magnetic resonance quantum computer. All of the balanced and constant functions were realized exactly. The results agree well with theoretical predictions and clearly distinguish the balanced functions from constant functions. Efficient refocusing schemes were proposed for the soft *z* pulse and *J* coupling, and it is shown that the thermal equilibrium state gives the same answer as the pure state for this algorithm.

PACS number(s): 03.67.Lx

A quantum computer, which was just a theoretical concept, has been realized recently by nuclear magnetic resonance (NMR). Several methods have been proposed such as ion trap [1,2], quantum dot [3,4], cavity quantum electrodynamics [5,6], and Si-based nuclear spins [7] to realize quantum computers, but NMR [8] has given the most successful results. Several quantum algorithms have been implemented by NMR quantum computers [9–13] among which the Deutsch-Jozsa (DJ) algorithm [14] has been studied most because it is the simplest quantum algorithm that shows the power of a quantum computer over a classical one. Most quantum algorithms, including the DJ algorithm, have been implemented only for functions of one and two bits. The successful implementation of a quantum algorithm depends heavily on the number of basic operations that increases with the number of qubits due to finite coherence time. Moreover, more than two-bit operations require more than two-body interactions that do not exist in nature. It is possible, though not easy, to avoid such interactions but it increases again the number of total basic gates, and coherence may break down during the computation. There have been few works that have performed real three-bit operations [15] so far.

The DJ algorithm determines whether an *n*-bit binary function

$$f:\{0,1\}^n \mapsto \{0,1\} \tag{1}$$

is a constant function that always gives the same output or a balanced function that gives 0 for half the inputs and 1 for the remaining half. The DJ algorithm gives the answer with only one evaluation of the function while a classical algorithm requires $(2^{n-1}+1)$ evaluations in the worst case. The function is realized in quantum computation by unitary operation

$$U|x\rangle|y\rangle = |x\rangle|y \oplus f(x)\rangle, \tag{2}$$

where x is an n-bit argument of the function and y is one bit. If $|y\rangle$ is in the superposed state, $(|0\rangle - |1\rangle)/\sqrt{2}$, then the result of the operation,

$$U|x\rangle\left(\frac{|0\rangle-|1\rangle}{\sqrt{2}}\right) = (-1)^{f(x)}|x\rangle\left(\frac{|0\rangle-|1\rangle}{\sqrt{2}}\right) \tag{3}$$

carries information about the function encoded in the overall phase. If $|x\rangle$ is also prepared in the superposition of all its possible states, $(|0\rangle+|1\rangle+\cdots+|2^n-1\rangle)/\sqrt{2^n}$, by applying an n-bit Hadamard operator H to $|x\rangle=|0\rangle$, the relative phases of the 2^n states change depending on f. If f is a constant function, then the relative phases are all the same and additional application of H restores $|x\rangle$ to $|0\rangle$. If f is a balanced function, $|x\rangle$ cannot be restored to $|0\rangle$ by this operation. It is obvious that $|y\rangle$, being in the superposed state, $(|0\rangle-|1\rangle)\sqrt{2}$, plays a central role in the algorithm but it is redundant in the sense that its state does not change.

This redundancy is removed in the refined DJ algorithm [16], where the following unitary operator is used:

$$U_f|x\rangle = (-1)^{f(x)}|x\rangle. \tag{4}$$

It has been shown that U_f is always reduced to a direct product of single-bit operators for $n \leqslant 2$. In this case, the quantum algorithm solves the Deutsch problem in a classical way in the sense that qubits are never entangled as discussed in Ref. [16]. Therefore, meaningful tests of the DJ algorithm can occur if and only if $n>2$. Recently, a realization of the DJ algorithm for $n=4$ has been reported [17], but in that work, only one balanced function was evaluated and the corresponding U_f is reducible to a direct product of four single-bit operators. In this study, we investigated the refined DJ algorithm with three-bit arguments to find out the pulse sequences of U_f's and implemented the algorithm on an NMR quantum computer for all the functions.

There are ${}_8C_4=70$ balanced and two constant functions among all three-bit binary functions. We indexed the functions with their outputs $f(0)\cdots f(7)$, expressed as hexadecimal numbers. For example, f_{1E} denotes the function of which the outputs are given by $f(0)\cdots f(7)=00\,011\,110$. Note that $U_{f_x}=-U_{f_{FF-x}}$, where x is a hexadecimal number equal to or less than FF (FF is a hexadecimal number equal to 256). The difference of overall phase cannot be distin-

TABLE I. Sequences of realizable operators for U_f's corresponding to 35 balanced functions.

	Type-I
f_{0F}	$I_z(\pi)$
f_{33}	$S_z(\pi)$
f_{55}	$R_z(\pi)$
f_{3C}	$I_z(\pi)S_z(\pi)$
f_{66}	$S_z(\pi)R_z(\pi)$
f_{5A}	$R_z(\pi)I_z(\pi)$
f_{69}	$I_z(\pi)S_z(\pi)R_z(\pi)$
	Type-II
f_1	$I_z(\pi)S_z(-\pi/2)R_z(-\pi/2)J_{23}(\pi/2)$
f_{2D}	$I_z(\pi)S_z(\pi/2)R_z(-\pi/2)J_{23}(\pi/2)$
f_{3B}	$I_z(\pi)S_z(-\pi/2)R_z(\pi/2)J_{23}(\pi/2)$
f_{78}	$I_z(\pi)S_z(\pi/2)R_z(\pi/2)J_{23}(\pi/2)$
f_{36}	$S_z(\pi)I_z(-\pi/2)R_z(-\pi/2)J_{13}(\pi/2)$
f_{39}	$S_z(\pi)I_z(\pi/2)R_z(-\pi/2)J_{13}(\pi/2)$
f_{63}	$S_z(\pi)I_z(-\pi/2)R_z(\pi/2)J_{13}(\pi/2)$
f_{6C}	$S_z(\pi)I_z(\pi/2)R_z(\pi/2)J_{13}(\pi/2)$
f_{56}	$R_z(\pi)I_z(-\pi/2)S_z(-\pi/2)J_{12}(\pi/2)$
f_{59}	$R_z(\pi)I_z(\pi/2)S_z(-\pi/2)J_{12}(\pi/2)$
f_{65}	$R_z(\pi)I_z(-\pi/2)S_z(\pi/2)J_{12}(\pi/2)$
f_{6A}	$R_z(\pi)I_z(\pi/2)S_z(\pi/2)J_{12}(\pi/2)$
	Type-III
f_{4E}	$I_z(\pi/2)S_z(-\pi/2)J_{23}(\pi/2)J_{13}(\pi/2)$
f_{13}	$I_z(\pi/2)S_z(\pi/2)J_{23}(-\pi/2)J_{13}(\pi/2)$
f_{27}	$I_z(\pi/2)S_z(\pi/2)J_{23}(\pi/2)J_{13}(-\pi/2)$
f_{72}	$I_z(-\pi/2)S_z(\pi/2)J_{23}(\pi/2)J_{13}(\pi/2)$
f_{3A}	$S_z(\pi/2)R_z(-\pi/2)J_{12}(\pi/2)J_{13}(\pi/2)$
f_{53}	$S_z(\pi/2)R_z(\pi/2)J_{12}(-\pi/2)J_{13}(\pi/2)$
f_{35}	$S_z(\pi/2)R_z(\pi/2)J_{12}(\pi/2)J_{13}(-\pi/2)$
f_{5C}	$S_z(-\pi/2)R_z(\pi/2)J_{12}(\pi/2)J_{13}(\pi/2)$
f_{2E}	$I_z(\pi/2)R_z(-\pi/2)J_{12}(\pi/2)J_{23}(\pi/2)$
f_{47}	$I_z(\pi/2)R_z(\pi/2)J_{12}(-\pi/2)J_{23}(\pi/2)$
f_{1D}	$I_z(\pi/2)R_z(\pi/2)J_{12}(\pi/2)J_{23}(-\pi/2)$
f_{74}	$I_z(-\pi/2)R_z(\pi/2)J_{12}(\pi/2)J_{23}(\pi/2)$
	Type-IV
f_{17}	$S_z(\pi)J_{12}(\pi/2)J_{23}(\pi/2)J_{13}(-\pi/2)$
f_{1B}	$S_z(\pi)J_{12}(\pi/2)J_{23}(-\pi/2)J_{13}(\pi/2)$
f_{4D}	$S_z(\pi)J_{12}(\pi/2)J_{23}(\pi/2)J_{13}(\pi/2)$
f_{71}	$S_z(\pi)J_{12}(-\pi/2)J_{23}(\pi/2)J_{13}(\pi/2)$

guished in the experimental implementations. Therefore, there are 35 distinct unitary operators corresponding to the balanced functions and one operator corresponding to the constant functions. Since the unitary operator corresponding to the constant functions $U_{f_{00}}$ is just the unity matrix, there are 35 nontrivial and distinct U_f's to be implemented.

The NMR Hamiltonian of the weakly interacting three-spin system is given by

$$\mathcal{H}=\sum_{i}^{3}\Delta\omega_i I_{iz}+\sum_{i<j}^{3}\pi J_{ij}2I_{iz}I_{jz} \tag{5}$$

in the rotating frame, where I_{iz} is the z component of the angular momentum operator of spin i. The first term represents the precession of spin i about the z axis due to the chemical shift $\Delta\omega_i$ and the second term, the spin-spin interaction between spin i and j with coupling constant J_{ij}. This Hamiltonian provides six unitary operators, $I_{iz}(\theta)=\exp[-\imath\theta I_{iz}]$ and $J_{ij}(\theta)=\exp[-\imath\theta 2I_{iz}I_{jz}]$. In combination with $I_{iz}(\theta)$, two other operators $I_{ix}(\theta)$ and $I_{iy}(\theta)$ produced by rf pulses can perform any single-bit operations. The coupling operator $J_{ij}(\theta)$ can be used to make a controlled-NOT operation. The combination of single-bit operations and controlled-NOT operations can generate any unitary operations [18].

Table I shows the sequences of the realizable operators for all the 35 nontrivial distinct U_f's. In the table, the notations I_1, I_2, and I_3 were replaced by I, S, and R, respectively, for convenience. Some of U_f's are not representable as a direct product of one- or two-qubit gates and require three-body interaction. The sequences of realizable operators in the table were obtained by following a general implementation procedure using generator expansion [19]. This method includes the coupling order reduction technique that replaces an n-body interaction operator for $n>2$ by two-body ones. It is noticed that all U_f's consist of the operators of the single-spin rotations about the z axis and spin-spin interactions only. From now on, we call pulses corresponding to these operators the soft z pulse and J coupling, respectively.

The balanced functions are classified into four types depending on the number of $J_{ij}(\theta)$'s included in their operation sequences. It is easy to see that no qubits are entangled in type-I functions and therefore, obviously they are not the cases of meaningful tests. In type-II functions, only two qubits out of three are entangled. So, type-II functions can be said to be the stepping stones to meaningful tests. In type-III and -IV functions, all three qubits are entangled and the functions of these types can be tested only by a three-bit quantum computer. Therefore, the realization of type-III and -IV functions demonstrates the true quantum parallelism. It is worthwhile to note, however, that the realization of these functions by NMR does not demonstrate the true quantum parallelism because small NMR systems cannot produce entangled states [20]. Each sequence in Table I is not unique for a given function but we believe that the sequences are optimal ones for implementation of the refined DJ algorithm.

The whole operation sequence for implementation of the refined DJ algorithm is given by H-U_f-H-D to be read from left to right. The first and second H's were realized by hard $\pi/2$ and $-\pi/2$ pulses about the y axis, respectively. Since the readout operation D can be realized by a hard $\pi/2$ pulse about the y axis, the second H and D cancel each other to make the sequence H-U_f.

The superposed input state is generated by the Hadamard operation on the pure state $|0\rangle$. Therefore, it is usually necessary to convert the thermally equilibrated spin state into the effective pure state. In the case of the refined DJ algorithm, however, the thermal equilibrium state gives the same results with the pure state except signal intensity. The deviation density matrix of the thermal equilibrium state ρ_{th} is approximated by

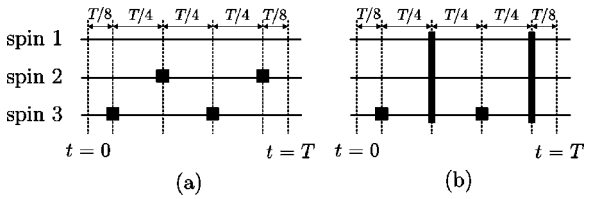

FIG. 1. Refocusing schemes for (a) $I_z(\theta)$ and (b) $J_{12}(\theta)$. Short and long bars represent soft and hard π pulses, respectively. The angle θ can be changed by adjusting the length of evolution time T.

$$\rho_{\mathrm{th}}=I_{1z}+I_{2z}+I_{3z} \tag{6}$$

for the Hamiltonian of Eq. 5, and the density matrix of $|0\rangle$, ρ_{p}, is given by

$$\rho_{\mathrm{p}}=I_{1z}+I_{2z}+I_{3z}+2I_{1z}I_{2z}+2I_{2z}I_{3z}+2I_{1z}I_{3z}+4I_{1z}I_{2z}I_{3z}$$
$$=\rho_{\mathrm{th}}+\Delta\rho. \tag{7}$$

The hard $\pi/2$ pulse for H transforms terms of ρ_{th} into single-quantum coherence and terms of $\Delta\rho$ into multiple-quantum coherence [21]. Since the sequences for U_f's consist of only the soft z pulse(s) and J coupling(s) that are dependent only on the z components of spin angular momentums, U_f's do not change the order of quantum coherence. As single-quantum coherence is only observable, the required answer can be read off from the thermal equilibrium input as well as from a pure-state input. In general, the thermal-equilibrium state gives the same answers with the pure state if the operation sequence after the first Hadamard operator does not change the order of quantum coherence.

The soft z pulse and J coupling were implemented by the time evolution under the Hamiltonian of Eq. (5) with refocusing π pulses applied at suitable times during the evolution period. Since the refocusing π pulse has the effect of time reversal, it can be used to make one term in the Hamiltonian evolve while the other terms ''freeze'' [22–24]. We optimized these *refocusing schemes* as illustrated in Fig. 1. Figure 1(a) shows the refocusing scheme for the soft z pulse on spin 1, and (b) that for the J coupling between spin 1 and 2 as examples. The evolution time T, is $\theta/\Delta\omega_i$ for the soft z pulse and $\theta/(\pi J_{ij})$ for the J coupling. Previous schemes divide the evolution period into eight periods and require six pulses, or suffer from the two-spin effect (TSETSE) [25,26] because soft pulses exciting more than one but not all spins were used. Since the difficulty of the experiment increases exponentially with an increasing number of pulses, especially soft pulses, our scheme greatly enhances the possibility of successful implementation. Axes of successive π pulses were chosen in the way to cancel imperfections of pulses. For example, four π pulses in Fig. 1(a) were applied along the y, $-y$, $-y$, and y axes, respectively.

In our experiment, ^{13}C nuclear spins of 99% carbon-13 labeled alanine in D_2O solvent were used as qubits. NMR signals were measured by using a Bruker DRX300 spectrometer. The chemical shifts of three different carbon spins are about 5670, -3780, and -6380 Hz, and coupling constants J_{12}, J_{23}, and J_{13} are 54.06, 34.86, and 1.30 Hz, respectively. Protons were decoupled during the whole experiments.

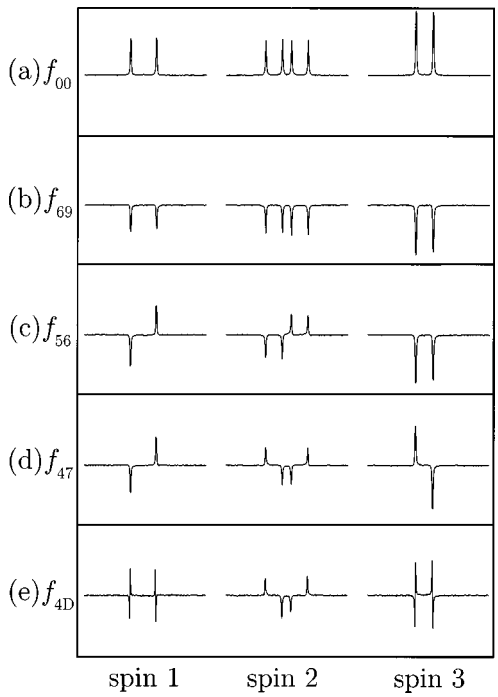

FIG. 2. The spectra of (a) the initial superposed state and the final states for (b) f_{69}, (c) f_{56}, (d) f_{47}, and (e) f_{4D}. The x axis represents frequency increasing from right to left. All the spectra are drawn in the same horizontal and vertical scales.

Gaussian-shaped soft π pulses were about 2 ms in length. The length of the total pulse sequence was about 450 ms in the worst case.

We implemented all the 35 balanced and one constant functions exactly. Figure 2 shows the initial superposed state and the results for the four functions belonging to different types shown in Table I. All the spectra are drawn in the same horizontal and vertical scales. The lines of the spectra for the remaining functions also indicate as clearly as ones in the figure whether they are positive or negative. The balanced functions are distinguished from the constant function because some of the lines are negative. The peaks of spin 1 and 3 show up as doublets in Figs. 2(b), 2(c), and 2(d), while that of spin 2 is quartet because J_{13} is very small compared to J_{12} and J_{23}. Figure 2(e) shows, however, that the peaks of spin 1 and 3 are in fact quartet also. They look like dispersive doublets because the neighboring lines split a little by J_{13} have different signs. These results agree well with the theoretical predictions obtained from

$$\mathrm{Tr}(I_+ e^{-\imath\mathcal{H}t/\hbar}\rho e^{\imath\mathcal{H}t/\hbar}), \tag{8}$$

where ρ is the density matrix transformed by the operation sequence H-U_f from ρ_{th} and $I_+=I_x+\imath I_y$.

Our refocusing schemes decrease the length of the total pulse sequence and, therefore, reduce signal decay due to decoherence. Imperfection of soft pulses and off-resonance effects of hard pulses are thought to be the main sources of the phase error and the decay of signal amplitude of some lines. These imperfections are more serious in the J coupling

than in the soft z pulse because out-of-phase multiplets are produced in the former while in-phase multiplets are produced in the latter. Therefore, it is very important to calibrate soft pulses exactly, especially for long sequences.

In summary, we implemented the complete refined DJ algorithm with three-bit arguments, which involves entanglement. All the operations were realized by the time evolution under Hamiltonian with refocusing π pulses. The operation sequences best for our implementation were found using generator expansion. Experimental pulse sequences were made as simple as possible by using the thermal equilibrium state and the new refocusing schemes.

This work was supported by the Brain Korea 21 project.

[1] J.I. Cirac and P. Zoller, Phys. Rev. Lett. **74**, 4091 (1995).
[2] C. Monroe, D.M. Meekhof, B.E. King, W.M. Itano, and D.J. Wineland, Phys. Rev. Lett. **75**, 4714 (1995).
[3] A. Barenco, D. Deutsch, A. Ekert, and R. Jozsa, Phys. Rev. Lett. **74**, 4083 (1995).
[4] D. Loss and D.P. DiVincenzo, Phys. Rev. A **57**, 120 (1998).
[5] Q.A. Turchette, C.J. Hood, W. Lange, H. Mabuchi, and H.J. Kimble, Phys. Rev. Lett. **75**, 4710 (1995).
[6] P. Domokoss, J.M. Raimond, M. Brune, and S. Haroche, Phys. Rev. A **52**, 3554 (1995).
[7] B.E. Kane, Nature (London) **393**, 133 (1998).
[8] N. Gershenfeld and I.L. Chuang, Science **275**, 350 (1997).
[9] I.L. Chuang, L.M.K. Vandersypen, X. Zhou, D.W. Leung, and S. Lloyd, Nature (London) **393**, 143 (1998).
[10] I.L. Chuang, N. Gershenfeld, and M.G. Kubinec, Phys. Rev. Lett. **80**, 3408 (1998).
[11] J.A. Jones and M. Mosca, J. Chem. Phys. **109**, 1648 (1998).
[12] J.A. Jones, M. Mosca, and R.H. Hansen, Nature (London) **393**, 344 (1998).
[13] N. Linden, H. Barjat, and R. Freeman, Chem. Phys. Lett. **296**, 61 (1998).
[14] D. Deutsch and R. Jozsa, Proc. R. Soc. London, Ser. A **439**, 553 (1992).
[15] Y.S. Weinstein, S. Lloyd, and D.G. Cory, e-print quant-ph/9906059.
[16] D. Collins, K.W. Kim, and W.C. Holton, Phys. Rev. A **58**, R1633 (1998).
[17] R. Marx, A.F. Fahmy, J.M. Myers, W. Bermel, and S.J. Glaser, e-print quant-ph/9905087.
[18] A. Barenco, C.H. Bennett, R. Cleve, D.P. DiVincenzo, N. Margolus, P. Shor, T. Sleator, J. Smolin, and H. Weinfurter, Phys. Rev. A **52**, 3457 (1995).
[19] J. Kim, J.-S. Lee, and S. Lee, Phys. Rev. A **61**, 032312 (2000).
[20] S.L. Braunstein, C.M. Caves, R. Jozsa, N. Linden, S. Popescu, and R. Schack, Phys. Rev. Lett. **83**, 1054 (1999).
[21] E. Ernst, G. Bodenhausen, and A. Wokaun, *Principles of Nuclear Magnetic Resonance in One and Two Dimensions* (Oxford Univ. Press, Oxford, 1987).
[22] N. Linden, H. Barjat, R.J. Carbajo, and R. Freeman, Chem. Phys. Lett. **305**, 28 (1998).
[23] D.W. Leung, I.L. Chuang, F. Yamaguchi, and Y. Yamamoto, e-print quant-ph/9904100.
[24] J.A. Jones and E. Knill, e-print quant-ph/9905008.
[25] N. Linden, E. Kupče, and R. Freeman, Chem. Phys. Lett. **311**, 321 (1999).
[26] E Kupče, J.-M. Nuzillard, V.S. Dimitrov, and R. Freeman, J. Magn. Reson., Ser. A **107**, 246 (1994).